Pol. J. Environ. Stud. Vol. 34, No. 5 (2025), 5001-5015
DOI:*10.15244/pjoes/190656* ONLINE PUBLICATION DATE: 2024-11-18

Original Research

Hygroscopic Flare-Based Cloud Seeding to Increase Rainfall Over Lake Toba

Samsul Bahri[1*], Heru Widodo[1], Mahally Kudsy[1], Sunu Tikno[1], Tukiyat Tukiyat[1], Muhamad Djazim Syaifullah[2], Ardhi Adhary Arbain[2], Jon Arifian[2], Sutrisno Sutrisno[2]

[1]Research Center for Limnology and Water Resouces, National Research and Innovation Agency (BRIN), Indonesia
[2]Directorate for Laboratory Management, Research Facilities, and Science and Technology Park, National Research and Innovation Agency (BRIN), Indonesia

Received: 28 November 2023
Accepted: 30 June 2024

Abstract

The declining North Sumatra's Lake Toba water level caused PT Inalum to request BRIN to replenish the lake through cloud seeding to meet the electrical power production. Cloud seeding was conducted from April 1 to 29, 2021, during the transition of rainy and dry seasons. The Piper-Cheyenne aircraft equipped with CoSAT-1000 hygroscopic flares departed Silangit Airport for the daily seeding missions. The seed clouds are selected carefully to meet seeding criteria using radar monitoring. Evaluation of activity results using rainfall data taken from GSMaP data using the Target Only Statistical Method. Actual and historical rainfall data (2001–2020) are taken from GSMaP data. According to this study, precipitation has increased by 36.3%. The spatial distribution of rainfall demonstrates an upward trend, with greater values observed in the eastern region of Lake Toba. Cloud seeding has also increased Lake Toba's level by 8.5 cm. In addition, it has also produced an additional inflow of 5.29 m^3/second, equivalent to a water volume of 13,254,624 m^3, comparable to 15,905,548.80 kWh. It is hoped that the outcomes of this work will help provide food and energy security by supplying water to dams in Indonesia.

Keywords: Rainfall, convective cloud, cloud seeding, hygroscopic flare, cloud condensation nuclei

Introduction

Cloud seeding is a process used to artificially enhance the formation of clouds and induce more extensive precipitation. It is a method to increase rainfall by introducing hygroscopic particles, such as sodium chloride or ice nuclei particles, such as silver iodide or other cold materials, into the cloud during precipitation [1]. Cloud seeding is also defined as the activity of injecting chemical compounds into the atmosphere to change the properties of the atmosphere [2]. Cloud modifying activities are generally carried out by sprinkling particles of seeding material into the air to add CCN or ice nuclei to increase rainfall [3]. Aerosol particles can serve as CCNs to form cloud droplets [4]. Aerosol particles in the atmosphere act as efficient CCNs and play an essential role in creating warm clouds [5].

A warm cloud is a convective cloud with a cloud-top temperature higher than 0°C. Consequently, the processes

*e-mail: sams001@brin.go.id
Tel.: +62 815 899 0411

in the cloud occur in the liquid phase. The cloud process transforms into rain through collision and coalescence [6]. Convective or warm cloud seeding can be conducted using seeding material such as hygroscopic flares or powdered salt. Hygroscopic seeding involves hygroscopic seeding material to expedite precipitation by stimulating the activation of less hygroscopic natural particles and promoting the creation of larger water droplets [7].

Cold cloud has a temperature below the freezing level (less than 0°C) where rainfall occurs through the "Glaciogenesis-Process." Cold cloud seeding involves the introduction of aerosols into vertically growing clouds to modify the formation of cloud droplets and enhance precipitation [8]. Cold cloud seeding involves introducing silver iodide aerosol into a supercooled liquid cloud to accelerate the formation of ice crystals. These ice crystals grow in size and velocity, eventually leading to rainfall reaching the ground [9]. Evidence of the effects of cloud seeding can be gathered from flights near the tops of cold clouds and observation with remote sensing satellites, penetrating aircraft, and radars before and during seeding. The evidence shows the process of supercooled liquid water droplets, which rapidly freeze and crystallize into ice. The droplets collide with each other and fall as rain, a phenomenon not occurring in unseeded supercooled droplets [10]. Previous experiments have demonstrated that cold cloud seeding occurs during precipitation formation, specifically focusing on using supercooled water solutions in cold clouds [1]. Research on glaciogenic cloud seeding done in the Kupang region of Nusa Tenggara Province using liquid carbon dioxide as the seeding ingredient results in a 40% increase in rainfall [11].

By strategically considering local weather patterns, cloud seeding can mitigate water scarcity in specific regions [12]. Economic growth, rapid population growth, and direct and indirect impacts of climate variability resulting in increased pressure on water resources have made cloud seeding technology viable for improving water supply [13]. Several nations have employed cloud-seeding technology to augment precipitation in their desert areas and tackle domestic issues [14].

The evaluation of additional rainfall resulting from cloud seeding activities can be conducted using one of the following statistical methods: target alone, target control, and double ratio. To assess the outcomes of augmented precipitation from cloud seeding, employ the statistical technique known as target control [15]. Consequently, it is necessary to create and construct a network of meteorological monitoring devices, including rain gauges, wind direction indicators, and wind speed meters, within the designated region of operation [16]. Efforts to overcome the delicate problems of cloud seeding, namely how to calculate cloud seeding results and obtain statistical evidence of increased rainfall, as well as steps that must be established to optimize cloud seeding techniques, have been carried out [17]. Weather modification experts have developed various evaluation methods for calculating cloud seeding results in recent decades. The evaluation method includes setting a conservation equation for a two-dimensional convective cloud model to simulate the effect of silver iodide seeding on increased rainfall from convective clouds [18].

Nowadays, cloud seeding is not only used to increase rainfall but also to reduce cloud cover, clean the air of pollutants, extinguish fires, store water ice in mountainous areas during the winter, and divert rain away from flood-prone metropolises, which gives rise to claims of 'losses' from areas receiving unwanted rain [19]. Cloud seeding experiments to reduce air pollution have been carried out in the Korean region several years ago. The effects of cloud seeding include an increase in radar reflectivity, cloud concentration, and greater precipitation particle diameter after seeding, especially PM10 concentrations (particles with a size of ≤ 10 μm), which tend to decrease in cloud seeding areas [20]

Cloud seeding carried out in Indonesia is mainly intended to increase the volume of water in reservoirs or lakes with an electrical energy generation industry (PLTA) and reduce the impact of disasters due to forest and land fires. Several companies that have hydroelectric energy generation industries in Indonesia, such as PT Inalum (Persero), PT Inco, Tbk (now PT Vale, Tbk), PT Jasa Tirta 1, PT Jasa Tirta 2, and PT PLN (Persero) have utilized this cloud seeding technology to maintain the water level of lakes and reservoirs so that their hydropower plants can operate optimally. PT. Vale, Tbk has utilized flare-based cloud seeding technology using aircraft and ground-based generator towers as an integrated part of water resources management in the Larona catchment area, South Sulawesi Province [21]. Cloud seeding, done from a static platform on the surface or a ground-based generator tower, has the disadvantage that it can only seed clouds that move and approach the Tower. The results are certainly not optimal, but the cost is relatively cheaper. Cloud seeding with dynamic platforms such as airplanes has the advantage that planes can search and find seedable clouds far away and in large numbers. The results are undoubtedly optimal, but the cost is relatively more expensive. A drone cloud seeding platform has also recently been developed, which utilizes remote and in situ real-time data and makes cloud seeding operations low-cost, safe, and optimal. Its development continues to be improved to be implemented in the future [22]. Cloud seeding using an aircraft platform is more effective than using a generation platform from the ground, such as ground-based generators, rockets, or other types of artillery [23].

The timing of cloud seeding is a factor that significantly impacts the success of rain enhancement; the right time will yield the best results and vice versa. Other factors that affect the success of cloud seeding and challenges faced during activities include how to ensure that support from Ground Support Equipment (GSE) to fly an aircraft at all times is fulfilled, communication between the Pilot and Flight Scientist onboard the plane is smooth, global data support (gradient wind analysis, sea surface temperature, pressure, and satellite imagery) is always available, and smooth access to weather radar data and local weather data is maintained. One of the crucial factors that determine the success of cloud seeding is the assessment of the climatological conditions of the region to assess the trend of potential cloud development, that is, seedable clouds, cloud types, liquid water content, the lifetime of clouds, and other to allow us to assess the prospects and profitability of the experiments carried out whether the benefits outweigh the costs incurred [24].

Due to Lake Toba's falling water level, which threatens electricity production at the Asahan Power Plant, PT Inalum (Persero) requested the implementation of a cloud seeding research project above Toba Lake. Cloud seeding is performed using the flare technique. This paper presents cloud seeding experiments on convective clouds with hygroscopic flares in the catchment area of Lake Toba, North Sumatra Province, using Piper Cheyenne II aircraft from April 1 to 29, 2021.

Experimental Procedures

Cloud seeding activities are evaluated using two approaches, first from the aspect of rainfall and second from the element of water flow that comes into the inflow of Lake Toba's catchment area. Rainfall measurement in the catchment area of Lake Toba was carried out in 2 ways. First, it is based on the hourly satellite data of the JAXA Global Rainfall Watch (JAXA/EORC). This is obtained through the internet from ftp://hokusai.eorc.jaxa.jp site. The hourly GSMaP data is collected 24 hours daily to get daily rainfall data. Similarly, monthly rainfall data in the catchment area can be obtained from daily data. Second, rainfall data is obtained from rain gauge stations owned by BPPT, BMKG, and PT Inalum (Persero) at locations scattered in the Lake Toba catchment area (Fig. 1).

This experiment calculated the additional rainfall based on GSMaP data, considering the satellite data could detect precipitation in all Lake Toba catchment areas. In addition, GSMaP data can be obtained continuously online. Rain measuring data is owned by BPPT, BMKG, and PT Inalum (Persero), which only exists in 13 locations. Measurement data from these 13 measuring sites are not used in calculating additional rainfall because there is no historical data from rains in the same month as the activity. Therefore, the additional rainfall calculations in this study use GSMaP data and are compared with GSMaP data. Instead, the GSMaP historical data is used. The method used in assessing the addition of rainfall resulting from cloud seeding activities over Lake Toba uses a target-only statistical evaluation method [25]. The added rain is calculated from the difference between the actual and historical rainfall values as follows [26]:

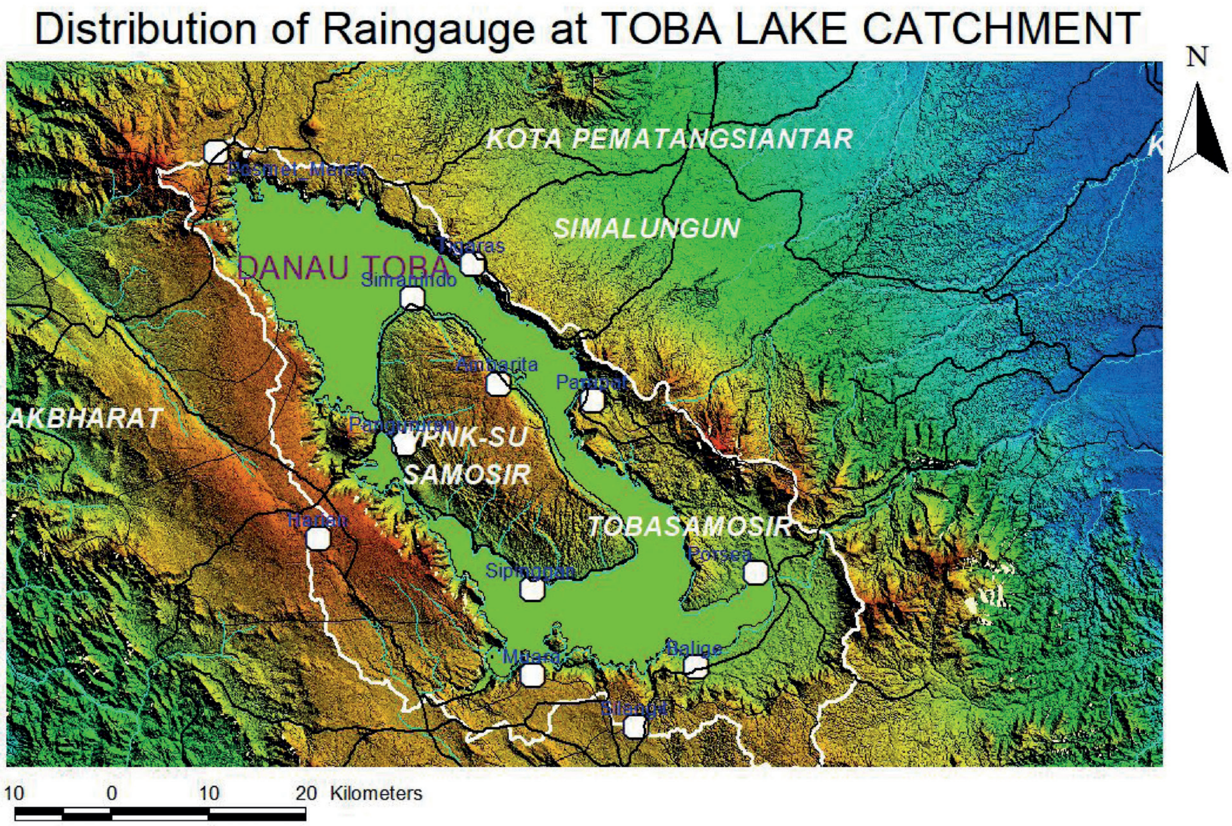

Fig. 1. Distribution map of rainfall measuring locations (white dots) owned by BPPT, BMKG, and PT Inalum (Persero) in the catchment area of Lake Toba.

$$\delta = \frac{(\alpha - \theta)}{\theta} \times 100\%$$

where: δ = added rainfall (%)
α = actual precipitation (mm)
θ = historical precipitation (mm)

Rainfall data was used in evaluating results using rainfall data from the GSMaP JAXA satellite (Fig. 2). The added precipitation is calculated by comparing actual rain data with historical rain data for ten years (2001–2010) in the same month (April).

In evaluating the results of cloud seeding using inflow data, the management of PT Inalum (Persero) has provided preliminary information that the Lake Toba inflow baseline in April 2021 was 138.60 m^3/second. The added inflow during the activity is obtained from the actual inflow magnitude minus the prediction inflow (baseline of the management of PT. Inalum). The prediction inflow is agreed upon or determined before the start of the project. Table 1 is used as a reference to see whether there is an increase in inflow or a decrease after the cloud seeding experiment. Therefore, if the inflow increases, the additional volume of water entering Lake Toba can be calculated, and the cloud seeding experiment is declared victorious. The extra volume of water is then converted into electrical power production, which is an advantageous value for PT Inalum (Persero). Based on information from the PT Inalum (Persero) management, 1 m^3 of water can produce an electrical energy of 1.2 kWh.

The clouds seeded over the Lake Toba area are clouds with vertical growth, such as Cumulus (Cu), Cumuli forms, and orographic clouds. Orographic clouds and cumuli form are found above the catchment area of Lake Toba. These clouds contain a lot of water vapor and produce precipitation. Cu and orographic clouds are suitable clouds, with cloud base heights between 4000 and 4500 feet and cloud top elevations between 10,000 and 13,000

Table 1. Additional inflow, water volume, and electricity production during cloud seeding activities in the Lake Toba catchment area.

Duration (days)	29
Baseline Inflow (m^3/sec)	138.60
Actual Inflow (m^3/sec)	143.89
Inflow Addition (m^3/sec)	5.29
Water Volume (m^3)	13,254,624
Electrical energy (kWh)	15,905,548.80

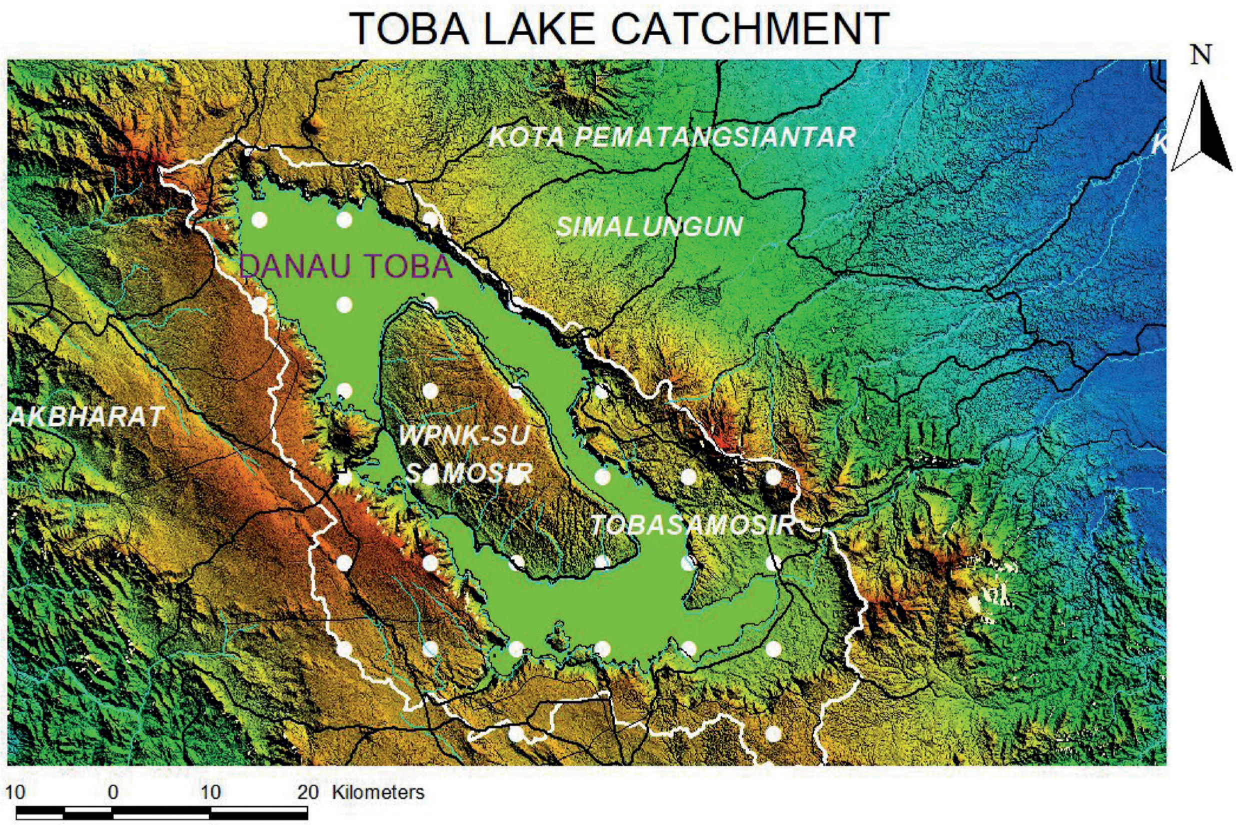

Fig. 2. GSMaP_NRT data calculation grid in the Lake Toba catchment area. The solid white line and white dots represent the catchment area and grid of GSMaP_NRT, respectively.

feet. Clouds with this criterion are also called potential clouds or suitable clouds. Cloud growth is monitored for easy detection from weather radar, and the radar guides decisions to carry out cloud-seeding flights.

This research activity used 1 unit of Piper Cheyenne II turboprop aircraft registration number PK-TMC owned by BPPT, which had rack-mounting flares installed on both aircraft wings (Fig. 3). Using the Piper Cheyenne II aircraft in cloud seeding activities with this flare technique is because the load is relatively light. Previous cloud seeding experiments used larger Casa 212 aircraft because the seeding material was an enormous amount of salt powder (thousands of kilograms). The Piper Cheyenne II aircraft has advanced navigation systems such as weather radar and Global Positioning System (GPS). Weather radar helps identify the location and potential of clouds to seed. GPS helps record the position and track the aircraft on the map where the cloud execution has been carried out.

This was the first time cloud seeding in Lake Toba used the flare technique. The seeding flare material used is a CoSAT-1000 (Cloud Seeding Agent Tube) hygroscopic flare made by PT Pindad (Persero) Indonesia, with as many as 169 flares burnt. The main composition of CoSAT 1000 chemicals is $CaCl_2$ as its hygroscopic agent, with $KClO_4$ (Potassium Perchlorate) as an oxidizer and Mg (Magnesium) as fuel and binder. The weight size of 1 CoSAT flare is about 1 kg. The particle size distribution produced by CoSAT 1000 for particles with a diameter of 0.7–1.1 microns as much as 25.15%, a diameter of 1.1–2.1 microns as much as 44.2%, and particles with a diameter of 2.1–3.3 microns as much as 13.58%. [27]. Flare CoSAT 1000 was chosen for the first time in weather modification over Lake Toba because it wanted to see the effect of the size of the fine seeding material used (0.7–3.3 microns) on the results of cloud seeding. So far, the material used has a particle size above 70 microns. CoSAT 1000 also marks a milestone

Fig. 3. Convective Cloud Seeding on Lake Toba in April 2021 using Piper Cheyenne II PK-TMC aircraft and CoSAT-1000 hygroscopic flares.

in Indonesia's release history from dependence on imported flare products.

Cloud seeding flight procedures are carried out when weather conditions are favorable. If the weather conditions on that day are unfavorable, cloud-seeding flights are not executed. Daily flights are conducted from Sisingamangaraja XII International Airport in Silangit to the catchment area of Lake Toba with flying altitudes between 5000 to 8000 feet according to the height of convective clouds found over Lake Toba. Flight operation procedures are carried out after weather data has been analyzed. The analyzed data include surface air temperature, pressure, humidity, wind direction, speed, cloud and sinope-scale weather data, and satellite imagery. Data analysis to determine opportunities or indications of cloud growth in the target area and to define the supply of clouds from outside that enter the target area. Synop data and satellite imagery were analyzed to determine the global influences on local and regional weather conditions. The results of data analysis are used to design flight strategies, such as where the execution area is and when the right time to fly is. Cloud growth conditions in the target area can be known by utilizing C-band radar data from the Meteorology and Geophysics Agency operated in Kualanamu and Nias. Information on suitable clouds in the catchment area of Lake Toba as a result of radar monitoring is considered, as well as the decision to fly immediately and not to fly.

Results

Table 2 shows the calculated results of cloud seeding using hygroscopic flares to increase rainfall in the Lake Toba Catchment Area, which has increased rainfall by 36.3% (Table 2). The average rainfall is 12.04 mm, with a standard error of the mean of 2.03 mm and a standard deviation of 11.12 mm. Rainfall data in Table 2 is obtained from the precipitation recorded by the rain gauges, while the historical rainfall data is obtained from GSMaP for 2001–2010. A better descriptive statistical evaluation of this cloud seeding result is made by comparing the April 2021 rainfall of 361.2 mm against GSMaP data with a period range of 2001–2020 scores of $t(19) = -8.38$, $p = 0.001$ at 95% significant level. This test shows that the rainfall produced during the cloud seeding period is significantly different (i.e., more important) from historical rainfall (205.8 ± 82.8 mm) in 2001–2020.

Table 2. Added rainfall during cloud seeding.

Parameters	Rainfall
Actual precipitation	361.2 mm
Historical rainfall 2001–2020 (from GSMaP)	265.0 mm
Precipitation addition	96.2 mm
Added rainfall gain	36.3 %

The rainfall in the catchment area of Lake Toba resulting from cloud seeding is relatively evenly distributed, with an intensity between 200 mm and 500 mm. The spatial distribution of rainfall shows an increase; where the value is getting to the eastern region of Lake Toba, the spatial rainfall value is getting higher (Fig. 4 a). After the seeding period, there is a strong tendency for spatial precipitation to increase in the catchment area. Figure 4 (b) plots the rainfall difference between April and March 2021.

Cloud seeding has produced high regional rain in the Lake Toba catchment area, 361.2 mm based on GSMaP data (Table 3) and 195.0 mm based on rainfall measurement data (Table 4). The rainfall value obtained with GSMaP is much higher than that obtained with the rain gauges because the existing gauges cannot cover the entire target area. The highest rain intensity occurred

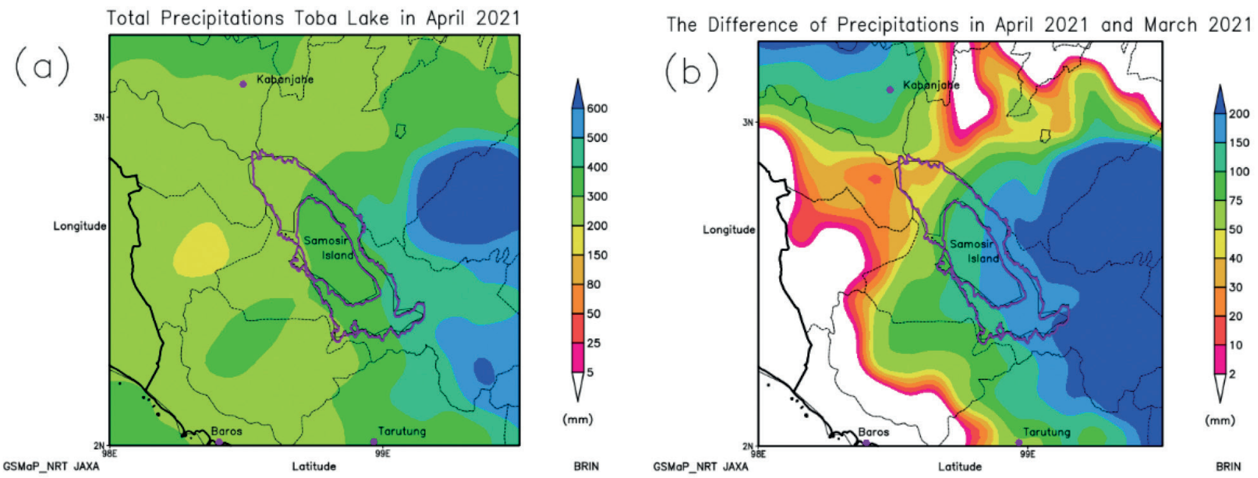

Fig. 4. Total Precipitation in the catchment area of Lake Toba for April 2021 (derived from GSMaP_NRT JAXA). (a) total precipitation in April 2021 and (b) the difference in precipitation between April 2021 and March 2021, respectively.

on April 26, 2021, at 37.1 mm (GSMaP data) and 19.5 mm (rainfall measurement). Figure 5 compares the patterns of rainfall intensity and fluctuations between historical (yellow line) and actual (blue line), which looks different; for historical rainfall, the intensity and fluctuation of rainfall look less fluctuating or flat, while for actual rain, it looks very fluctuating rainfall intensity. This demonstrates the influence of cloud seeding on the rainfall.

Cloud seeding also has succeeded in increasing the water level of Lake Toba by 8.5 cm (Table 5). The actual inflow is 143.89 m^3/second, and the natural or predicted inflow is 138.60 m^3/second, so this cloud seeding activity has produced an inflow increase of 5.29 m^3/second. The added inflow is identical to the volume of water of 13,254,624 m^3 and is equivalent to the added electrical energy production of 15,905,548.80 kWh (Table 1). It should be mentioned here that according to the management of PT Inalum (Persero), 1 m^3 of water is equivalent to 1.2 kWh of electrical energy [25].

Discussion of Results

Table 6 shows the flight recapitulation of Piper Cheyenne II from April 1 to 29, 2021. The tropical cyclones (TC) during this period can be seen in this table: TC Serodja and TC Surigae. TC Serodja was detected from April 5 to 8, 2021, in the Indian Ocean, and TC Surigae was seen from April 12 to 24, 2021, in the South China Sea (Fig. 6). A tropical cyclone generally influences weather conditions and rainfall, especially around the tropical cyclone. The influence of tropical storms can cause high rainfall in the surrounding area for hundreds of kilometers [28]. Research on extreme precipitation due to tropical cyclones in mainland China and the relationship between excessive rain due to tropical storms and ENSO has been carried out [29]. The study results showed that 76% of the 1673 tropical cyclones analyzed contributed to heavy rainfall on the Philippine mainland along the northwest coast of Luzon [30].

It is assumed that TC Serodja and Surigae affect the wind and air masses that enter the catchment area of Lake Toba because the air mass is attracted by the cyclone's tail, thus changing the region's wind gradient pattern. In other words, the growth of convective clouds in the catchment area of Lake Toba experiences obstacles. The distance between the tropical cyclone's location and Lake Toba's catchment area is hundreds of kilometers. Hence, its influence is not so significant on the growth of local convective clouds in the catchment area. Based on field observations, in the period of the appearance of the two cyclones, the development of convective clouds in the catchment area of Lake Toba still exists so that cloud seeding flights can still be carried out. However, on April 3, April 4, and April 10, 2021, when these three days were not in the period of tropical cyclone appearance, cloud seeding flights were not carried out because, throughout the day, there was no potential for cloud growth in the catchment area (Table 6). It needs further study if, in the period, the presence

Table 3. Rainfall from GSMaP data in the Lake Toba catchment area during cloud seeding activities from 1 – 30 April 2021.

Date	Rainfall (mm)
April 1, 2021	0.23
April 2, 2021	0.92
April 3, 2021	24.52
April 4, 2021	0.26
April 5, 2021	6.14
April 6, 2021	15.05
April 7, 2021	15.05
April 8, 2021	29.84
April 9, 2021	0.32
April 10, 2021	0.26
April 11, 2021	3.96
April 12, 2021	16.65
April 13, 2021	3.45
April 14, 2021	2.35
April 15, 2021	26.96
April 16, 2021	8.87
April 17, 2021	0.89
April 18, 2021	7.31
April 19, 2021	12.85
April 20, 2021	6.09
April 21, 2021	30.24
April 22, 2021	18.24
April 23, 2021	21.94
April 24, 2021	19.48
April 25, 2021	30.58
April 26, 2021	37.11
April 27, 2021	4.60
April 28, 2021	0.48
April 29, 2021	7.48
April 30, 2021	9.02
Total	361.2

Table 4. Rainfall measurement data in the Lake Toba catchment area for 1–30 April 2023. *Numbers 1 to 16 are the names of rainfall measuring stations as follows: 1: ARG Gurgur Balige, 2: AWS Parapat, 3: AWS Simanindo, 4: Daily ARG, 5: AWS Sipinggan, 6: AWS Ambarita, 7: Silangit Airport, 8: AWS Balige, 9: AWS Muara, 10: AWS Ajibata, 11: Pangururan Rain Post, 12: AWS Tigaras, 13: Posmet Porsea, 14: Posmet Merek, 15: Silaen, 16: Lumban Lobu.*

Rainfall Measurement																	
	Rainfall Station																Average
Date	1	2	3	4	5	6	7	8	9	10	11	12	13	14	15	16	
1	0.6	-	0.2	0.4	0.0	2.2	3.2	0.0	0.6	0.0	0.0	0.2	0.0	0.0	0.0	1.0	0.6
2	0.4	-	0.0	0.4	0.0	0.0	0.1	0.0	0.0	0.4	1.0	0.2	0.0	0.3	0.0	0.0	0.2
3	0.2	-	0.0	1.8	0.9	0.3	3.7	0.0	0.4	0.0	2.0	0.2	6.0	2.0	0.0	0.0	1.2
4	0.0	-	0.0	0.0	0.0	0.1	0.0	0.0	0.0	0.0	0.0	0.0	0.0	0.4	0.0	0.0	0.0
5	0.0	3.2	0.0	0.0	0.0	0.0	0.0	0.0	0.0	4.3	0.0	0.0	0.0	0.0	27.0	0.0	0.5
6	2.0	22.8	1.3	4.0	0.0	0.3	2.5	0.0	2.4	24.8	3.0	0.2	2.4	24.8	10.0	0.0	5.8
7	1.6	0.4	4.3	0.2	0.1	0.0	2.1	1.1	0.0	0.4	7.0	0.2	6.2	0.4	27.0	18.0	3.3
8	19.4	11.6	3.5	0.4	10.7	16.4	1.1	12.9	0.0	8.3	2.0	-	14.5	29.8	0.0	5.0	10.8
9	1.4	0.0	0.1	0.2	8.1	1.0	6.6	0.0	4.0	0.1	0.0	0.2	0.0	1.0	0.0	0.0	1.4
10	0.0	0.2	0.0	0.8	0.1	2.3	-	0.0	0.0	0.0	0.0	0.2	0.0	3.2	0.0	0.0	0.5
11	0.8	22.8	0.0	0.8	0.2	0.4	9.0	0.2	0.1	16.6	0.0	26.6	TTU	5.5	0.0	12.0	6.3
12	3.6	7.6	7.9	7.8	1.2	33.3	4.0	10.7	13.6	5.1	1.0	26.6	8.5	27.5	11.0	5.0	10.9
13	0.8	0.2	0.0	1.8	0.4	11.8	2.0	9.1	3.8	2.2	13.0	0.0	4.7	0.5	3.0	1.0	3.4
14	0.0	26.0	0.0	0.2	11.3	4.1	TTU	12.7	0.0	22.5	0.0	17.6	0.0	2.2	0.0	0.0	6.4
15	10.8	24.2	33.4	20.0	25.2	19.0	24.0	6.0	25.4	15.6	11.0	2.2	29.0	38.2	8.0	8.0	18.8
16	24.0	2.8	0.0	11.4	10.1	17.3	15.5	0.0	0.9	1.4	3.0	26.0	3.8	19.0	7.0	42.0	11.5
17	24.2	5.0	0.0	0.0	6.2	4.3	TTU	0.2	16.7	3.7	0.0	0.0	2.4	14.0	3.0	0.0	5.3
18	13.2	28.4	38.1	1.0	2.1	19.9	32.0	4.1	0.3	14.5	1.0	0.0	12.5	11.0	3.0	3.0	11.5
19	1.0	0.0	0.0	30.4	0.6	0.6	27.5	0.0	0.1	0.0	0.0	0.0	34.0	5.5	6.0	7.0	7.0
20	1.2	0.0	19.1	10.0	0.9	4.9	1.0	0.2	0.2	2.3	17.0	3.8	4.8	8.0	0.0	0.0	4.6
21	24.2	19.4	0.7	2.4	14.9	2.8	20.0	10.6	0.0	12.9	4.0	6.0	28.5	18.0	5.0	96.0	16.6
22	1.6	0.6	2.0	6.2	0.1	0.0	10.5	0.9	0.2	4.6	4.0	0.0	7.5	2.0	9.0	5.0	3.4
23	0.0	1.6	0.0	0.2	0.0	0.2	TTU	0.1	0.1	0.0	4.0	0.0	3.0	0.0	18.0	3.0	2.0
24	11.2	17.2	8.5	2.6	0.1	9.1	16.0	11.5	0.1	13.8	5.0	10.6	13.6	13.0	11.0	7.0	9.4
25	0.2	9.6	2.2	0.0	0.0	5.2	TTU	2.3	0.2	7.2	7.0	0.0	4.7	0.0	18.0.0	8.0	4.3
26	30.6	1.6	15.5	19.6	0.0	21.7	25.5	10.9	0.2	27.0	32.0	30.0	19.2	42.0	13.0	24.0	19.6
27	21.0	4.2	0.1	0.2	0.1	16.1	17.8	9.1	0.3	1.6	0.0	1.6	0.7	8.0	3.0	7.0	5.7
28	0.0	0.0	0.0	0.2	0.0	0.0	0.0	0.0	0.6	0.0	0.0	0.0	TTU	38.0	0.0	0.0	2.6
29	30.6	18.6	0.0	26.7	0.0	0.0	13.0	14.0	0.5	0.0	14.0	0.0	-	-	14.0	14.0	9.8
30	2.3	46.6	2.0	4.0	0.0	2.8	4.7	0.3	0.4	30.2	14.0	32.2	-	-	-	-	11.6
Total																	195.0

Table 5. Recapitulation from the water level of Lake Toba, Effective Inflow and Outflow, during Cloud Seeding Activities on April 1 – 29, 2021.

Cloud Seeding Period	Water Level (MSL)	Average Effective Inflow (m^3/sec)	Average Outflow (m^3/sec)	Volume Inflow (Million m^3)	Volume Outflow (Million m^3)
Implementation Period 1 – 29 April 2021	Start: 903,243 End: 903,328 Δ Water Level: 8,5 cm	143.89	107.83	393.725	279.495

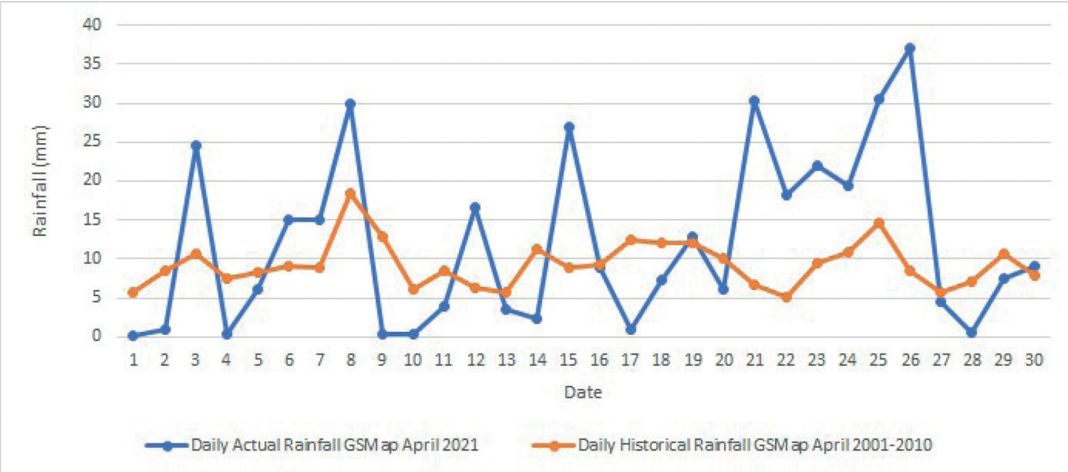

Fig. 5. Comparison between actual and historical rainfall for April 2021 based on GSMaP data.

of two tropical cyclones, Serodja (5 to April 8, 2021) and Surigae (12 to April 24, 2021), did not affect the growth of convective clouds in the catchment area of Lake Toba. Meanwhile, cloud seeding flight was not done because of no convective seedable clouds (April 3 and 4, 2021). The relationship between the presence of tropical cyclones and cloud-seeding flights is sometimes complicated. In such conditions, the decision to carry out flights depends on the pilot, the traffic controller, and the project coordinator. However, minimum weather conditions must always be met so that flights during tropical cyclones may be carried out. A tropical cyclone generally results in an 84% chance of increased rainfall [31].

Indian Ocean Dipole (IOD) is similar to the El-Niño Southern Oscillation (ENSO) but occurs in the Indian Ocean region west of Indonesia. IOD events are characterized by differences in Sea Surface Temperature (SST) anomalies between the Western tropical Indian Ocean (50°E – 70°E, 10°N – 10°S) and the Eastern tropical Indian Ocean (90°E – 110°E, 10°S – 0°). The IOD index is defined as the difference between SST anomalies in the Western Indian Ocean and the Eastern Indian Ocean region. A positive IOD Index value (+) indicates an increase in rainfall from normal (on the east coast of Africa and the western Indian Ocean). At the same time, on the Maritime Continent, Indonesia has decreased rainfall from the average, which causes drought [25]. The IOD Index value is negative (-), and the opposite condition occurs, which causes an increase in rainfall in the Indonesian Maritime Continent region. During the cloud seeding period, IOD conditions vary from adverse to neutral, which indicates that convective clouds in the target area have the potential to grow. Observations on the ground showed that convective clouds grow daily in the target area. The IOD index value in March 2021 was around -0.30 and reached a value of +0.32 at the end of April 2021 (Fig. 7). Based on the IOD index value data, during cloud seeding activities, there was a lot of convective cloud growth in the Lake Toba area. The relationship between ENSO and IOD is very consistent, and ENSO and IOD interact, so it is necessary to evaluate ENSO and IOD simultaneously [32]. ENSO, MJO, and IOD are very influential on local weather. Therefore, cloud seeding organizers are expected to understand weather fluctuations that can affect the success of cloud seeding.

Based on observations in the cloud seeding period, the sea surface temperature (SST) anomaly in the NINO 3.4 area was negative, while around Indonesian waters, it showed a positive abnormality. SST in the northern part of Sumatra ranges between 28.0°C and 31.0°C, while the anomaly of the SST ranges between -0.2°C and +1.0°C. The SST anomaly data analysis shows that the potential for evaporation and convective cloud formation in the catchment area of Lake Toba is still relatively high. Visual observations in Silangit City and at monitoring posts stationed in the towns of Porsea and Merek showed that convective clouds were growing daily in the target area. In

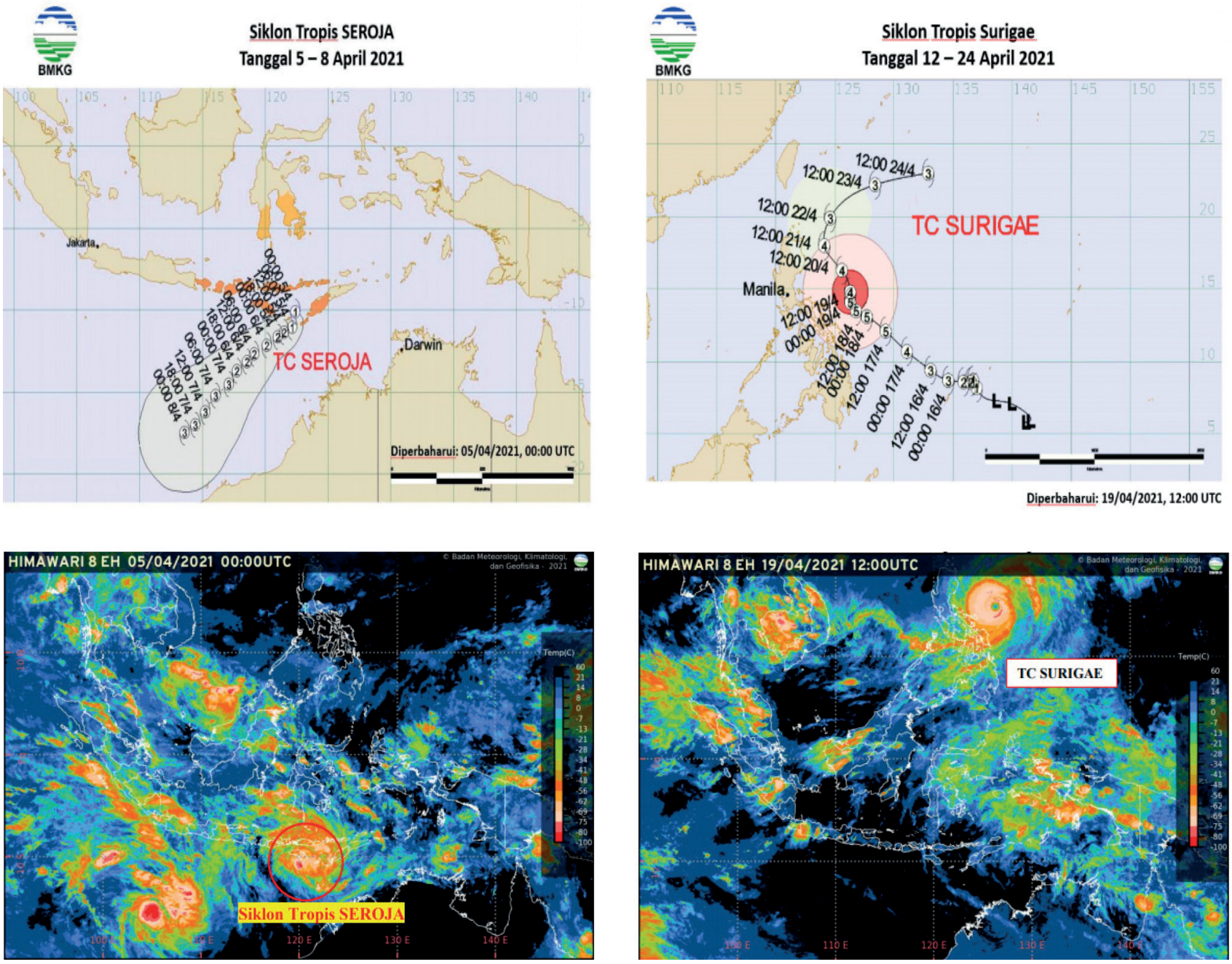

Fig. 6. Tropical Cyclones Serodja and Surigae on April 5, 2021, and April 19, 2021.

Table 6. Flight Recapitulation of Piper Cheyenne II PK-TMC in Cloud Seeding Activities in Lake Toba Catchment Area (1–29 April 2021).

Days to	Date	Flight	Flight Time (LT)	Seeding Area	Use Hygroscopic Flare (tube)
1	April 1, 2021	1	12.45–13.55	Southern, Southwest and Western parts of Lake Toba	4
2	April 2, 2021	1	11.00–12.10	Southern and Western parts of Lake Toba	5
3	April 3, 2021	Today, the cloud seeding flight was not carried out because there were no potential clouds in the Lake Toba area.			
4	April 4, 2021	Today, the cloud seeding flight was not carried out because there were no potential clouds in the Lake Toba area.			
5	April 5, 2021	1	13.45–15.05	Northern, Central, and Southern parts of Lake Toba	5
6	April 6, 2021	1	13.40–15.05	Northern, Central, and Southern parts of Lake Toba	7
7	April 7, 2021	1	13.10–14.45	Northern, Central, and Southern parts of Lake Toba	7
8	April 8, 2021	1	13.05–14.40	Northern, Central, and East parts of Lake Toba	8

Days to	Date	Flight	Flight Time (LT)	Seeding Area	Use Hygroscopic Flare (tube)
9	April 9, 2021	1	13.45–15.15	Northern, Central, and Southern parts of Lake Toba	6
10	April 10, 2021	Today, the cloud seeding flight was not carried out because there were no potential clouds in the Lake Toba area.			
11	April 11, 2021	1	12.20–13.50	Eastern, Southern, Central, and Northern Lake Toba	8
12	April 12, 2021	1	11.00–12.35	Central, Southeast, and Southern Parts of Lake Toba	6
		2	14.35–15.35	Southeast, South, Southwest, and Central of Lake Toba	6
13	April 13, 2021	1	12.25–13.50	Northern, Central, and Southern parts of Lake Toba	7
14	April 14, 2021	1	14.00–15.40	Central, North, East, South, and West of Lake Toba	9
15	April 15, 2021	1	11.50–13.30	Central, East, Southeast, and South of Lake Toba	8
16	April 16, 2021	1	13.45–15.45	Northern, Northeastern, Eastern, Southeast, and Central Parts of Lake Toba	10
17	April 17, 2021	1	13.20–14.45	Central, North, East, and Southern Parts of Lake Toba	8
18	April 18, 2021	1	14.05–15.40	Northern, East, Southeast, and Central Parts of Lake Toba	8
19	April 19, 2021	Today, the cloud seeding flight was not carried out because the aircraft was not airworthy (due to technical problems)			
20	April 20, 2021	Today, the cloud seeding flight was not carried out because the aircraft was not airworthy (due to technical problems)			
21	April 21, 2021	1	10.50–12.40	Northeast, Southeast of Lake Toba	5
		2	13.30–15.05	Central, Northeast, South, and Southwest of Lake Toba	6
22	April 22, 2021	1	13.00–14.55	Central, East, Southeast, and South of Lake Toba	6
23	April 23, 2021	1	14.15–15.50	Central, North, East, South of Lake Toba	5
24	April 24, 2021	1	11.00–12.45	North, Central, East, and South of Lake Toba	4
		2	14.40–16.00	Southern Part of Lake Toba	4
25	April 25, 2021	1	13.00–14.40	Central, Northeast, East of Lake Toba	5
26	April 26, 2021	1	12.50–14.05	Western, Central, and Northern Parts of Lake Toba	6
27	April 27, 2021	1	10.50–12.40	Northeast, Southeast of Lake Toba	5
28	April 28, 2021	1	12.25–14.00	Northern, Central, and Eastern parts of Lake Toba	5
29	April 29, 2021	1	11.45–13.25	Northern, East, South of Lake Toba	5

this case, the influence of SST is not so significant on cloud growth in the catchment area of Lake Toba because every day, cloud growth begins to be seen around 11:00 until late afternoon. According to rain patterns and cycles, the location of Lake Toba North Sumatra province is included in Region B. In Region B, where the division of Indonesia is linked to rain patterns and cycles, the influence of ENSO on Region B is less intense than in Areas C and A [33]. The relationship between the ENSO phenomenon and the rise of surface air temperatures in Southeast Asia that occurred during the extreme event in April 2016 has been investigated, and a strong relationship between ENSO and temperature rise in Southeast Asia where the contribution is estimated to be 29% due to regional warming and 49% due to the combined impact of the ENSO phenomenon [34]. The Pacific Ocean, Atlantic Ocean, and Indian Ocean are three important oceans for understanding climate variability. The interaction of the atmosphere and sea

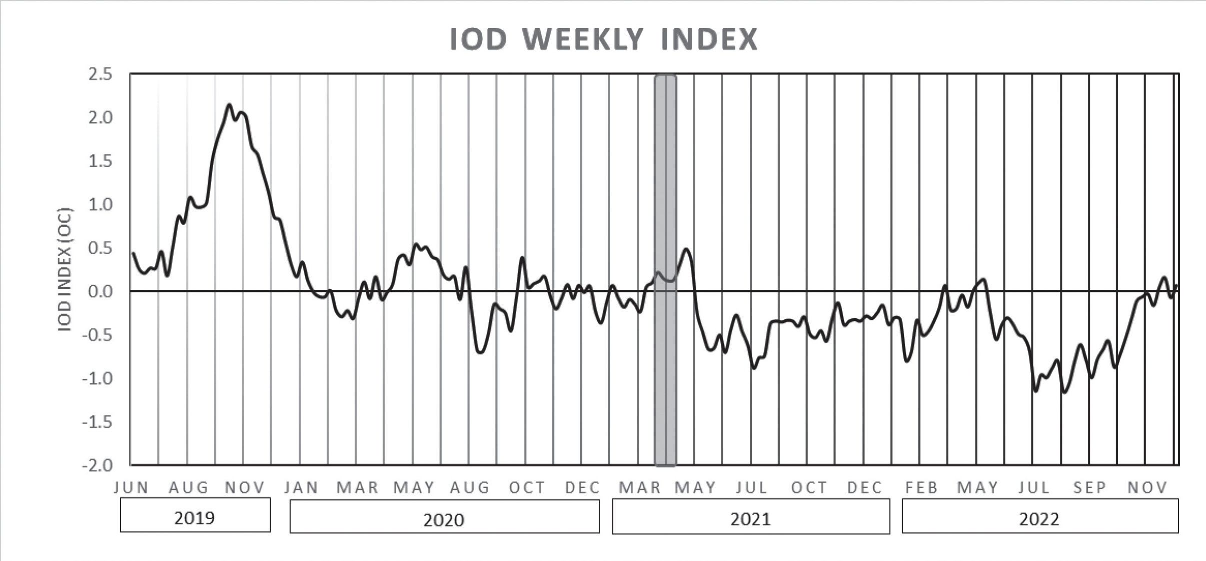

Fig. 7. Indian Ocean Dipole Index values from June 2019 until December 2022 (plotted from data source: http://www.bom.gov.au/clim_data/IDCK000072/iod_1.txt, downloaded on Dec 2023), the vertical shaded line indicates Cloud Seeding Operation period.

in the Pacific, Atlantic, and Indian Ocean regions can initiate climate variability, where the Pacific Ocean, as the home of ENSO, affects other oceans through atmospheric bridges and oceanic Indonesian throughflow (ITF), the Indian Ocean which produces Kelvin waves, and the North Atlantic SST Mid-latitude which can affect climate variability in the Pacific [35]. Studies have also tested how climate models' responses to the Pinatubo volcano eruption are associated with the early phase of the El Niño-Southern Oscillation (ENSO), which could help reconcile inconsistencies among previous studies [36].

Madden Julian Oscillation (MJO) is a global phenomenon in the form of atmospheric waves at the equator that move eastward with periods varying around 40–50 days. The wave phase shows increasing and decreasing cloud growth activity; the increasing degree is negative Outgoing Longwave Radiation (OLR), and the decreasing phase is positive OLR. In mid-March 2021, the OLR anomaly value in the catchment area of Lake Toba was in unfavorable conditions. Then, it increased positively from early April to the end of April 2021 (Fig. 8). In April 2021, along with the time of cloud seeding, the OLR value in the catchment area of Lake Toba was positive (there was a decrease in cloud growth activity). However, in the field, there was convective cloud growth every day. These phenomena can be shown from flight activity that occurs every day and only for three days without observable convective cloud growth (Table 6). Further discussions need to be continued, such as the causes of quite strong convective cloud growth in Lake Toba's catchment area, even though the OLR data shows positive values.

The use of Piper Cheyenne aircraft for cloud seeding in Toba Lake is efficient, fast, and easy to operate compared to non-flare techniques or conventional methods using powder seeding materials. The flare tube can be installed on an aircraft in minutes and is ready to fly. Due to the fast loading process, the window of opportunity (cloud seeding in the lifetime period of cloud growth) is always fulfilled. Delivery of hygroscopic particles can be carried out on several clouds or in cloud groups because the aircraft can carry 24 hygroscopic flares in each flight. Flight operations also do not require labor, as in weather modification operations using conventional powder materials. Cloud seeding activities are directly controlled by Flight Scientist from the aircraft cabin using a button switch. The flare technique is more effective and efficient than conventional.

The cloud seeding powder technique uses NaCl powder seeding material that has been ground several times to smoothen the particle size. NaCl powder seeding material used in cloud seeding in Indonesia has a particle diameter size of 60–80 μm [37]. This seeding material is carried using a Cessna 208 Caravan or a Casa 212 aircraft, which can load approximately 1,000 kg per flight. This hygroscopic NaCl seeding material acts as a condensation core that initiates rain. The salt powder technique requires a large aircraft to transport salt powder that weighs thousands of kilograms. As a result, flight preparation takes a long time, approximately 1 hour to load.

In contrast, the hygroscopic flare technique uses seeding material with a particle diameter ranging from 0.7 to 3.3 μm; the preparation for the flight only takes 5 to 10 minutes to install the flare on the aircraft. Carrying hygroscopic flare for seeding only requires light aircraft like Piper Cheyenne or Pilatus Porter. Cloud seeding activities on Lake Toba use Piper Cheyenne II aircraft equipped with rack-mounting. A rack-mounting is a tube flare holder that can take 12 flares on the left wing and 12 on the right. Cloud seeding activities occur from April

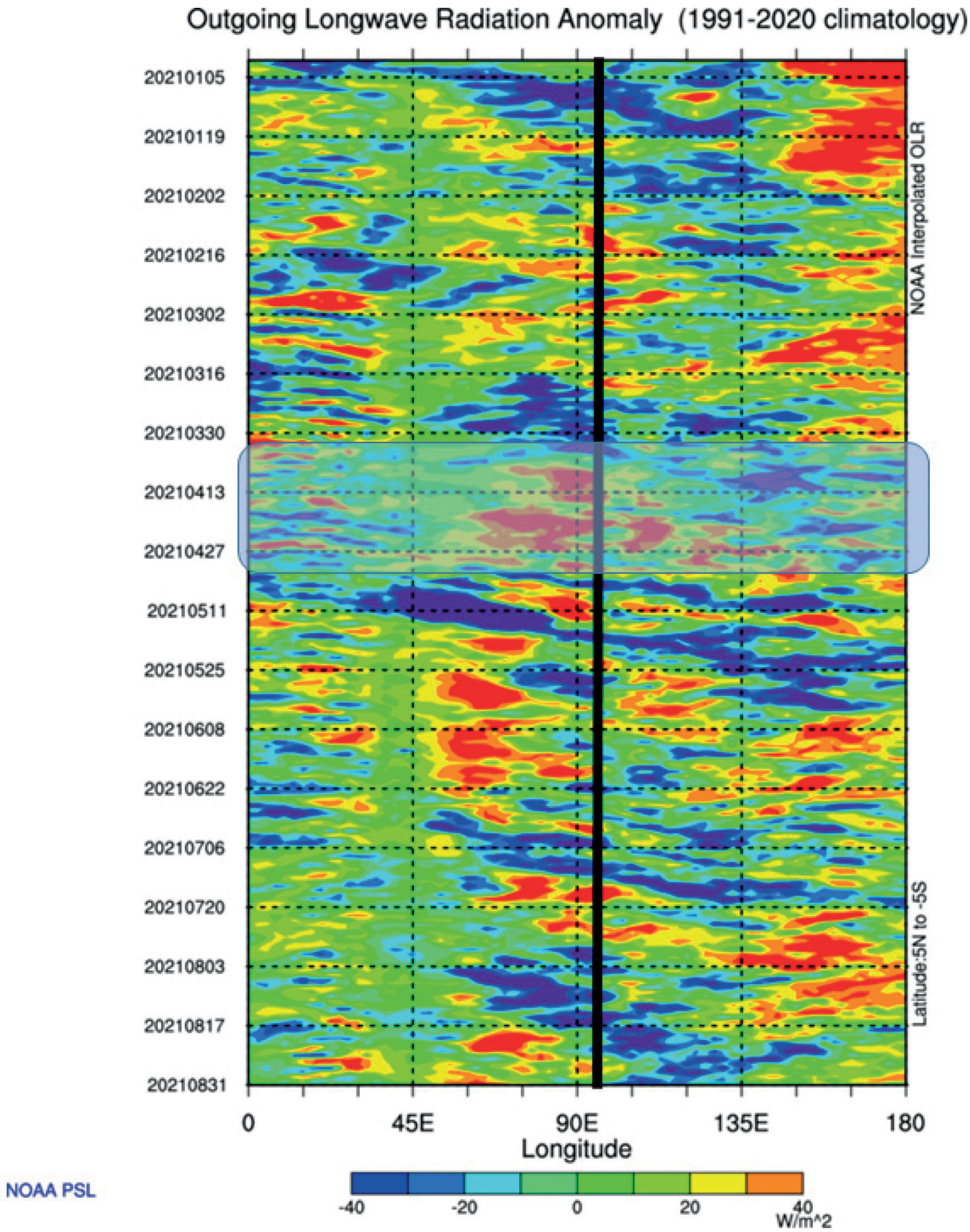

Fig. 8. Average OLR anomaly at average latitude 5ºN-5ºS from January until August 2021 computed from 1991–2020 climatology. Black vertical lines indicate the catchment area of Lake Toba, and transparency box shades indicate the Cloud Seeding Operation period (Data processing and plotting are facilitated by NOAA PSL Map Room, https://psl.noaa.gov/data/gridded/data.cpc_blended_olr-2.5deg.html).

1 to 29, 2021, and the seeding area covers the entire catchment area of Lake Toba (Table 6). Every day at 10:00 a.m. before the flight starts, a morning briefing involves meteorology, hydrology, physics, and chemistry experts to discuss the day's weather conditions and set the right flight time. The agenda in the morning briefing is quite interesting. In addition to discussing weather conditions and determining seeding time, researchers in the field of meteorology share knowledge about weather modification with flight crews so that the implementation of cloud seeding can be a complete unity between theory and its application in the field. Instead, the flight crew provides technical input and advice on how the cloud execution flight can be carried out safely and correctly.

In the morning briefing, convective cloud growth was monitored using radar data from BMKG in Medan

City and Nias Island. The criteria for seedable clouds are cumulus (Cu), cumulus-congestus (Cc), orographic clouds, and other vertically growing clouds that have cloud tops reaching 10,000 feet or more. Suppose seedable clouds have been detected on the radar monitor and are indicated in green, yellow, and red, and their position is within the catchment area of Lake Toba; flight preparations are immediately carried out. Hygroscopic flares were then mounted on the rack, with ten tubes (5 on the left wing and five on the right wing), while the flight crew communicated with the Tower via radio to ask permission to take off. It only takes about 5 to 10 minutes. Compare this with the salt powder technique. Herein lies the advantage of cloud seeding using the hygroscopic flare technique. Fast preparation time allows us to get many seedable clouds before the lifetime of the convective cloud ends or decays.

Conclusions

During the cloud seeding experiment on Lake Toba (April 1–29, 2021), the Piper Cheyenne II aircraft carried out 27 flights and spent 41 hours and 15 minutes flying. In the period 1–29 April 2021, there were five days of no cloud-seeding flight activities in the Lake Toba area. This is due to unfavorable weather conditions, convective clouds (April 3, 4, and 10, 2021), and technical damage to aircraft (April 19 and 20, 2021). During 27 cloud seeding flights, weather conditions and clouds were favorable for cloud seeding. The percentage of successful flight activities in cloud seeding missions within 29 days of activity was 82.8%. Cloud seeding experiments in Lake Toba have consumed 169 units of hygroscopic CoSAT-flares.

The cloud seeding work described above can produce additional water of 13,254,624 m^3, equivalent to electrical energy of 15,905,548.80 kWh in green energy. In addition, there was an increase in rainfall by 36.3%. Spatially, within the target area, rainfall is evenly distributed. Even though there are weather constraints, such as the presence of 2 tropical cyclones this time, the present cloud seeding works still get significant results to increase water reserves in Lake Toba.

This research has provided a new understanding of implementing cloud seeding in convective clouds in Indonesia, especially the use of hygroscopic flare seeding material, which has succeeded in increasing rainfall and inflow in the catchment area of Lake Toba. This flare technique is convenient, the grain size is more controlled, and it only requires a little personal use in the field. Installation of flares on aircraft only takes a few minutes; with such a short installation time, cloud seeding flights can obtain cloud lifetime in the growing period for sowing (window opportunity). However, the implementation of flares in Indonesia must obtain permission from the government.

This research contributes significantly to the government of the Republic of Indonesia's success of food and energy security programs by providing water to many energy generation reservoirs (PLTA) in Indonesia and contributing to the SDGs program that is being widely campaigned, especially in the field of food and clean energy.

Acknowledgments

On this occasion, the author expresses his infinite gratitude to the Reviewer Team, to the Head of the Limnology and Water Resources Research Center BRIN, Dr. Hidayat, for his endless moral support, Board of Management PT Inalum (Persero), and to all friends in the Weather Modification research group for their support.

Conflict of Interest

There is no conflict of interest between the authors and other parties.

References

1. LOU X., SHI Y., SHAN Y.A. Numerical Simulation of CCN Impacts on Weather Modification Efficiency. Frontiers in Environmental Science, **11**, **2003**.
2. KORETSKY Z., VAN LENTE H. Technology phase-out as unraveling of socio-technical configurations: cloud seeding case. Environmental Innovation and Societal Transitions, **37**, 302, **2020**.
3. YUAN J., WU K., WEI T., WANG L., SHU Z., YANG Y., XIA H. Cloud seeding evidenced by coherent Doppler wind lidar. Remote Sensing, **13** (19), **2021**.
4. MARINESCU P., HEEVER S., HEIKENFELD M., BARRETT A., BARTHLOTT C., HOOSE C., ZHANG Y. Impacts of varying concentrations of cloud condensation nuclei on deep convective cloud updrafts — a multimodel assessment. Journal of the Atmospheric Sciences, **78** (4), 1147, **2021**.
5. JOSE S., NAIR V., BABU S. Anthropogenic emissions from South Asia reverses the aerosol indirect effect over the northern Indian ocean. Scientific Reports, **10** (1), **2020**.
6. RENGGONO F., KUDSY M., ADHITYA K., PURWADI P., BELGAMAN H.A., DEWI S., SYAHDIZA R., MULYANA E., ALDRIAN E., ARIFIAN J. Hygroscopic Ground-Based Generator Cloud Seeding Design; A Case Study from the 2020 Weather Modification in Larona Basin Indonesia. Atmosphere, **13** (6), **2022**.
7. GERESDI I., XUE L., CHEN S., WEHBE Y., BRUINTJES R., LEE J., TESSENDORF S. Impact of hygroscopic seeding on the initiation of precipitation formation: results of a hybrid bin microphysics parcel model. Atmospheric Chemistry and Physics, **21** (21), 16143, **2021**.
8. FRENCH J.R., FRIEDRICH K., TESSENDORF S.A., RAUBER R.M., GEERTS B., RASMUSSEN R.M., XUE L., KUNKEL M.L., BLESTRUD D.R. Precipitation formation from orographic cloud seeding. Proceedings of the National Academy of Sciences of the United States of America, **115** (6), 1168, **2018**.
9. FRIEDRICH K., IKEDA K., TESSENDORF S., FRENCH J., RAUBER R., GEERTS B., PARKINSON S. Quantifying snowfall from orographic cloud seeding. Proceedings of the National Academy of Sciences, **117** (10), 5190, **2020**.

10. LI D., ZHAO C., YUE Z., CAO L., SUN Y., COHEN J. Response of cloud and precipitation properties to seeding at a supercooled cloud-top layer. Earth and Space Science, **9** (9), **2022**
11. MARYADI A., TOMINE K., NISHIYAMA K. Some aspects of a numerical glaciogenic artificial cloud seeding experiment using liquid carbon dioxide over Kupang, Indonesia. . Journal of Agricultural Meteorology, **71** (1), 1, **2015).**
12. AL HOSARI T., AL MANDOUS A., WEHBE Y., SHALABY A., AL SHAMSI N., AL NAQBI H., AL YAZEEDI O., AL MAZROUI A., FARRAH S. The UAE Cloud Seeding Program: A Statistical and Physical Evaluation. Atmosphere, **12** (8), **2021**.
13. KHATRI K., POKHAREL B., STRONG C. Development of hydrologically-based cloud seeding suspension criteria in the western United States. Atmospheric Research, **262**, 105768, **2021**.
14. WONDIE M. Modeling cloud seeding technology for rain enhancement over the arid and semiarid areas of ethiopia. Heliyon, **9** (4), e14974, **2023**.
15. RAUBER R.M., GEERTS B., XUE L., FRENCH J., FRIEDRICH K., RASMUSSEN R.M., TESSENDORF S.A., BLESTRUD D.R., KUNKEL M.L., PARKINSON S. Wintertime Orographic Cloud Seeding — A Review. Journal of Applied Meteorology and Climatology, **58** (10), 2117, **2019**.
16. ZHENG W., MA H., ZHANG M., XUE F., YU K., YANG Y., YIN X. Evaluation of the first negative ion-based cloud seeding and rain enhancement trial in china. Water (*Switzerland*), **13** (18), 2473, **2021**.
17. WU X., YAN N., YU H., NIU S., MENG F., LIU W., SUN H. Advances in the evaluation of cloud seeding: statistical evidence for the enhancement of precipitation. Earth and Space Science, **5** (9), 425, **2018**.
18. REN J., ZHANG W., KOU M., MA Y., ZHANG X. A numerical study of critical variables on artificial cold cloud precipitation enhancement in the Qilian mountains, China. Atmosphere, **14** (7), 1086, **2023**.
19. TANIKA L., WAMUCII C., BEST L., LAGNEAUX E., GITHINJI M., NOORDWIJK M. Who or what makes rainfall? Relational and instrumental paradigms for human impacts on atmospheric water cycling. Current Opinion in Environmental Sustainability, **63**, 101300, **2023**.
20. KU J., CHANG K., CHAE S., KO A., RO Y., JUNG W., LEE C. Preliminary results of cloud seeding experiments for air pollution reduction in 2020. Asia-Pacific Journal of Atmospheric Sciences, **59** (3), 347, **2023**.
21. PRASETIO A., ASHAR A. Operation and water management of dam cascade system, Available online: https://www.e3s-conferences.org/articles/e3sconf/abs/2022/13/e3sconf_cigb2022_03022/e3sconf_cigb2022_03022.html (accessed on 27 November 2022), **346**, 03022, **2022**.
22. DEFELICE T., AXISA D. Modern and prospective technologies for weather modification activities: developing a framework for integrating autonomous unmanned aircraft systems. Atmospheric Research, **193**, 173, **2017**.
23. HOSARI T., MANDOUS A., WEHBE Y., SHALABY A., SHAMSI N., NAQBI H., FARRAH S. The UAE cloud seeding program: a statistical and physical evaluation. Atmosphere. Atmosphere *(Basel)*, **12** (8), **2021**.
24. ABSHAEV A. Assessment of cloud resources and potential for rain enhancement: case study — Minas Girais State, Brazil. Atmosphere, **14** (8), **2023**.
25. BPPT Laporan Akhir Pelaksanaan Teknologi Modifikasi Cuaca di Daerah Tangkapan Air Danau Toba Provinsi Sumatera Utara Tahun 2021 - Tahap I (Periode 1–29 April 2021). Jakarta, **2021**.
26. BEARE S., CHAMBERS R., PEAK S. Statistical modelling of rainfall enhancement Working Paper, Available online: https://ro.uow.edu.au/cssmwp/34 (accessed on 2 December 2023).
27. HARYANTO U., GUNAWAN D., HARSANTI D. The Development of Hygroscopic Cloud Seeding Flare In Indonesia: Evaluation and Measurement of Distribution Particles. Bali, **2011**.
28. KHOUAKHI A., VILLARINI G., VECCHI G. Contribution of tropical cyclones to rainfall at the global scale. Journal of Climate, **30** (1), 359, **2017**.
29. ZHANG Q., GU X., LI J., SHI P., SINGH V. The impact of tropical cyclones on extreme precipitation over coastal and inland areas of China and its association to ENSO. Journal of Climate, **31** (5), 1865, **2018**.
30. BAGTASA G. Contribution of tropical cyclones to rainfall in the Philippines. Journal of Climate, **30** (10), 3621, **2017**.
31. BAI L., WAN R., RONG G., YING M., JIN R. Climate trends in tropical cyclone-induced precipitation and wind over Shanghai. Tropical Cyclone Research and Review, **11** (3), 219, **2022**.
32. MCKENNA S., SANTOSO A., GUPTA A., TASCHETTO A., CAI W. Indian ocean dipole in CMIP5 and CMIP6: characteristics, biases, and links to ENSO. Scientific Reports, **10** (1), **2020**.
33. ALDRIAN E., SUSANTO R. Identification of three dominant rainfall regions within Indonesia and their relationship to sea surface temperature. International Journal of Climatology, **23** (12), 1435, **2003**.
34. THIRUMALAI K., DINEZIO P., OKUMURA Y., DESER C. Extreme temperatures in Southeast Asia caused by El niño and worsened by global warming. Nature Communications, **8** (1), 1, **2017**.
35. WANG C. Three-ocean interactions and climate variability: a review and perspective. Climate Dynamics, **53** (7), 5119, **2019**.
36. PREDYBAYLO E., STENCHIKOV G., WITTENBERG A., ZENG F. Impacts of a pinatubo-size volcanic eruption on ENSO. Journal of Geophysical Research Atmospheres, **122** (2), 925, **2017**.
37. BRIN L.P.T.M.C. Laporan Akhir Pelaksanaan Teknologi Modifikasi Cuaca Di Daerah Tangkapan Air Danau Toba Provinsi Sumatera Utara Tahap III. J37akarta, **2022**.